

# A Procedure to Quantify the Variability of Geotechnical Properties

Daiane Folle, João Felipe C. Leite Costa, Jair Carlos Koppe, André Cesar Zingano

**Abstract.** The geotechnical properties of soil should be considered for several civil engineering purposes. Geotechnical information is used for urban planning, environmental management, slope stability analysis, and foundation design, among others. Given the importance that geotechnical information assumes in several engineering applications, geotechnical mapping is deemed relevant. Methods for integrating field tests and quantifying estimate uncertainty in the construction of these geotechnical maps is preferably used in the decision-making process. A methodology to build this kind of maps is proposed based on geostatistical stochastic simulation. Maps covering an area of 4 km<sup>2</sup> were built, based on the information derived from 141 boreholes, where standard penetration tests (SPT) were carried out. Sequential Gaussian simulation was used for building these maps, since it reproduces data statistics and spatial continuity. The soil resistance to penetration of panels of 100 x 100 m<sup>2</sup> was estimated and the estimation error was calculated. The results demonstrate the appropriateness and usefulness of the methodology for mapping geotechnical attributes.

**Key words:** geotechnical mapping, geostatistical simulation, SPT, uncertainty analysis.

## 1. Introduction

Highly heterogeneous soils impose difficulties in defining geotechnical properties correctly. This heterogeneity influences the choice of a safety factor to be used in engineering projects. In some situations, the geotechnical engineer adapts previous experiences to tackle the new conditions encountered (Elkateb *et al.*, 2003). Morgenstern (2000) reported 70% of failure in case studies where local experience was used to define geotechnical parameters. On the basis of these results, the authors of this study stressed the necessity for the use of novel methodologies that can assess uncertainty associated with the estimated geotechnical properties.

Generally, 0.5 to 1% of the total budget is allocated to civil engineering projects for application in soil investigation. For safety reasons, the project engineer tends to overestimate the safety factor used in relation to the soil strength when there is incomplete or inadequate geotechnical information. Geotechnicians are aware of the necessity of an adequate soil investigation, including field and lab tests. Some applications require maps of relevant parameters, showing their values at unsampled locations with the respective estimation error. These maps provide both the spatial distribution of geotechnical properties and their degree of uncertainty for risk assessment.

Many projects are not properly investigated in geotechnical terms, mainly due to budget restrictions. This in-

complete geotechnical investigation leads to the use of interpolation techniques to infill values of relevant soil parameters at unsampled areas. The most used techniques include the polygon method, triangulation and weighting by inverse distance to a power. These methods do not provide the error associated to the estimate and are not proper methods to interpolate geological or geotechnical properties.

Over the past four decades, geostatistical methods have been used for estimating regionalized variables and the corresponding estimation error in mining and earth science (Matheron, 1963; Isaaks & Srivastava, 1989). Presently, these methods have been widely applied to other areas such as petroleum engineering, environmental and reclamation engineering, fishery, and, also, most recently in geotechnical engineering (Sturaro & Landim, 1996; Armstrong, 1998; Chilès & Delfiner, 1999; Phoon & Kulhawy, 1999; Folle, 2002; Folle, 2003).

This paper reports a practical geostatistical application in geotechnical engineering, where the variable mapped is derived from field tests used to characterize soil penetration resistance. The test used (SPT) is explained in the subsequent paragraphs and consists of a common index used for foundation design. The type of foundation for ordinary buildings (from 3 to up to 30 levels) and parameters such as type and length of the pile foundation are frequently based on these SPT results, geological information, and local experience (Pinto, 2000).

---

Daiane Folle, Civil Engineer, PhD. Student, Departamento de Engenharia de Minas, Universidade Federal do Rio Grande do Sul, Porto Alegre, RS, Brasil. e-mail: daiane.folle@ufrgs.br.

João Felipe C. Leite Costa, Mining Engineer, PhD, Departamento de Engenharia de Minas, Universidade Federal do Rio Grande do Sul, Porto Alegre, RS, Brasil. e-mail: jfelipe@ufrgs.br.

Jair Carlos Koppe, Mining Engineer and Geologist, DSc., Departamento de Engenharia de Minas, Universidade Federal do Rio Grande do Sul, Porto Alegre, RS, Brasil. e-mail: jkoppe@ufrgs.br.

André C. Zingano, Mining Engineer, DSc., Departamento de Engenharia de Minas, Universidade Federal do Rio Grande do Sul, Porto Alegre, RS, Brasil. e-mail: andrezin@ufrgs.br.

Submitted on April 17, 2007; Final Acceptance on September 29, 2008; Discussion open until April 30, 2009.

This study aims at providing better tools for soil characterization used in foundation engineering. Also, areas of high uncertainty in soil properties should be identified and selected for additional sampling, in order to reduce engineering risk. These uncertainty maps are frequently used in mining (Pilger, 2000; Pilger *et al.*, 2001; Souza *et al.*, 2004), geology (Leuangthong *et al.*, 2004), petroleum engineering (Attanasi & Coburn, 2004), and environmental applications (Costa & Koppe, 1999) and can be promptly adapted for geotechnical engineering.

Considering the information provided by Standard Penetration Tests (SPT) and their spatial variability, this study investigates the appropriateness of a geostatistical methodology to map the spatial distribution of geotechnical properties derived from the SPT test. The map can be generated at a dense grid using geostatistical simulation.

The simulation framework provides access to the risk associated to an estimate quantifying its uncertainty. In this study, sequential Gaussian simulation (sGs) (Isaaks, 1990) is used to generate multiple scenarios of geotechnical properties of the soil. A case study illustrates this methodology generating maps at a 100 x 100 m<sup>2</sup> panels from a data set comprising standardized penetration tests.

## 2. SPT Test

Soil resistance is deemed relevant for foundation engineering and Brazilian technical standards (NBR-6484, 1999) define the procedure to collect soil penetration resistance, where the test known as Standard Penetration Test (SPT) consists basically of drilling and sampling soils along the hole. Also, a Brazilian standard such as NBR-7250 (1982) depicts two tables associating  $N_{SPT}$  with soil types; one table refers to sand-type soil and the other to clay-type soils.

The study area was irregularly sampled by 141 boreholes, where SPTs were carried out (Fig. 1). The maximum depth for those drill holes is 26 m, and most of them have not reached the so-called impenetrable level.

Four main soil types were observed along these drill holes with a gradational change from one type to the other. From top to bottom, the soil types are: red clay of medium consistency, silty red clay with yellow stains and medium consistency, silty-sandy red clay with yellow stains and rigid consistency, and silty-sandy gray clay with pieces of weathered rock very rigid to hard in terms of consistency. In order to explain the origin of these soil types, the local geological settings is presented hereinafter.

## 3. Geological Settings

Generally, the geology of the area comprises basalt rocks, belonging to Serra Geral Formation (JKsg), and sandstones and psamites, associated to the Tupanciretã Formation (Tt). Both formations are included in the Paraná Basin (RadamBrasil, 1986). Figure 2 shows a simplified geological map of the region. Note that the area object of

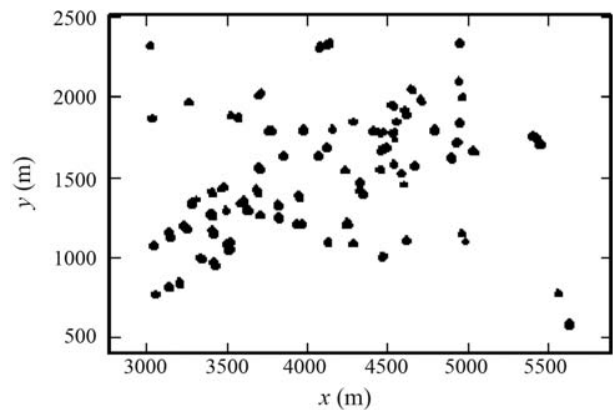


**Figure 1** - SPT data set location.

this study is covered by the basalts from the Serra Geral Formation.

Serra Geral Formation (JKsg) is composed of continental toleitic volcanic rocks, usually basalts, dacites, and rhyolites, with dikes and tubular bodies of diabase. Occasionally, there are lens and layers of intertraptic sandstones of the Botucatu Formation.

Tupanciretã Formation (Tt) covers part of the volcanic basaltic rocks at the north of the area. It is composed mainly of sandstones, usually reddish, sometimes yellow-green, with variable texture, poorly classified, eventually conglomeratic and composed essentially of quartz and, subordinately, feldspar weathered to kaolinite.

The soil weathered profile descriptions are related to the elevation, bedrock, and surface morphology. The morphology of the horizons is presented by Naime (1999) as:

(i) Horizon A well defined and subdivided, brown to reddish, formed mostly by clay, with some granular material, porous, hard when dry, plastic, and sticky when wet. There is a gradational contact to the lower horizon;

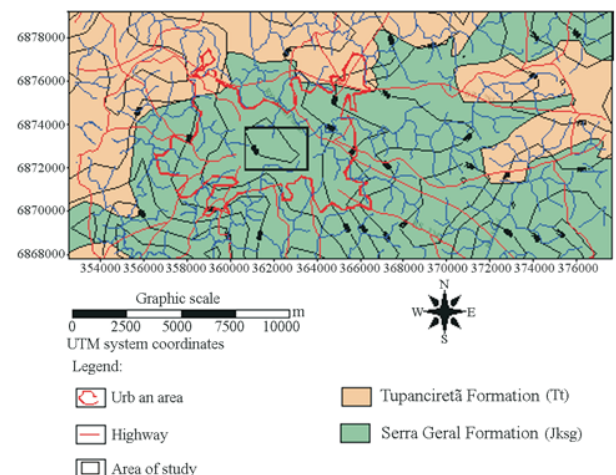


**Figure 2** - Geological Map for Passo Fundo region, depicting the area studied.

- (ii) Horizon B thick with subdivisions, dark red, clayey texture;
- (iii) Horizon C very deep, formed by weathered basalt.

All soil types described belong to the Passo Fundo unit (Fig. 3) and were developed over basaltic lithologies, forming brownish humic latosols, intermediate brownish and purple latosols, and latosols with developed B horizons.

The top soils show an excess of 1% of organic matter at 1 m depth, defining its humic characteristics. These soils are derived mainly from basic volcanic rocks and intermediate or acidic volcanic rocks.

Soils presented in the study area are reasonably homogeneous, with few morphological variations and inclusions derived from basaltic rocks. The topography is smoothly hilly with slopes within 8 to 10 % gradient. Locally, horizons B and C prevail.

#### 4. Data Set Description

The area sampled is formed by soils derived from the rock types mentioned before (mainly basalts). The sampling survey was carried out in the residual soils, consisting of 141 boreholes, and the samples were basically composed of clay material with few sand and gravel fragments. From the surface downwards to the bedrock, the residual soil is divided into three to four layers. The number of layers depends on the location. Each layer exhibits a specific range of  $N_{SPT}$  values.

Therefore, the data set was divided into subsets of similar soil typology and mean  $N_{SPT}$  values. The limits identifying each soil were proposed to be obtained by plotting the average of all  $N_{SPT}$  values at each depth (max 141) vs. the depth (Fig. 4). Note the sampling process, *i.e.*, SPT tests were conducted at every meter, starting immediately below the borehole collar. It is reasonable to assume a linear trend between  $N_{SPT}$  and depth. This linear trend is shown in the plot

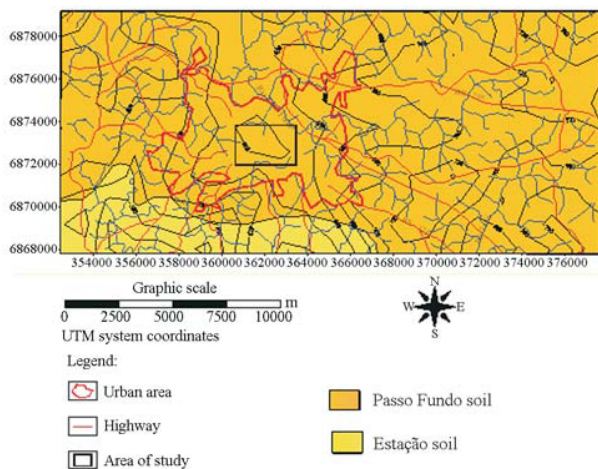


**Figure 3** - Soil Map for Passo Fundo region, depicting the area studied (compiled by Lemos, 1973).

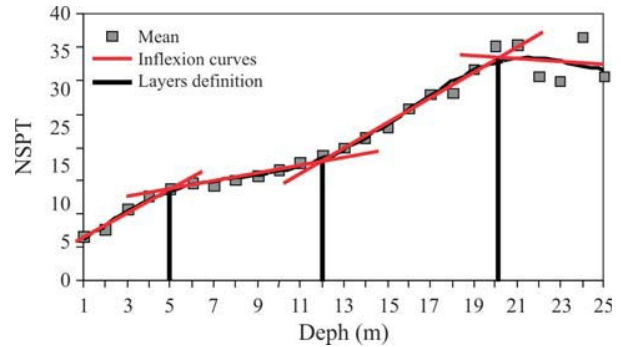


**Figure 4** - Depth x  $N_{SPT}$ . Slope variation helps in identifying geostatistical domains.

obtained (Fig. 4); however, four changes were observed in the slope of this trend. Each slope variation of the trend leads to a possible change in soil type, which in geostatistical terms would identify different stationary subsets.

Layers I and III are more erratic in terms of  $N_{SPT}$  values than layer II. The slope in the plot  $N_{SPT}$  vs. depth (Fig. 4) for layer II is distinct from the remaining layers. Layer II is also seen as a transitional zone from a low-resistance soil (layer I) and high-resistance soil (layer III).

Four groups (layers) were identified in Fig. 4 as follows: I (0 to 4.99 m), II (5 to 11.99 m), III (12 to 19.99 m), and IV (20 to 26 m). All these subsets were statistically analyzed and the results presented as follows (Fig. 5). Due to this criterion used to split the soil layers into geostatistical domains, the simulation will be run in 2D. The mean of  $N_{SPT}$  value for each soil interval intersected by each borehole is kept.

Figure 5 presents the histograms for the  $N_{SPT}$  values obtained for each soil layer. Histograms for layers I and II (Figs. 5a and 5b) show a positive asymmetry, layer III (Fig. 5c) is practically symmetric, and layer IV (Fig. 5d) presents a negative asymmetry caused by an excess of high values. These anomalous high values relate to the fact that various holes hit the bedrock. The last layer defines the contact with the bedrock. Many tests are known to be interrupted before reaching the bedrock (impenetrable by SPT). These asymmetric distributions (non-Gaussian) are typical of earth sciences datasets and are required to be normalized as it will be discussed hereinafter.

All layers have their  $N_{SPT}$  variograms modeled using a spherical variogram (Journel & Huijbregts, 1978). The main axes of anisotropy are, respectively, at N90E and N0. Equations (1) through (4) present the variogram models for layers I, II, III, and IV, respectively.

$$\gamma(h) = 3 + 22.70 \times Sph \left( \frac{N0^\circ}{492} + \frac{N90^\circ}{857} \right) \quad (1)$$

$$\gamma(h) = 6 + 70.40 \times Sph \left( \frac{N0^\circ}{547} + \frac{N90^\circ}{821} \right) \quad (2)$$

$$\gamma(h) = 10 + 75.90 \times Sph \left( \frac{N0^\circ}{757} + \frac{N90^\circ}{556} \right) \quad (3)$$

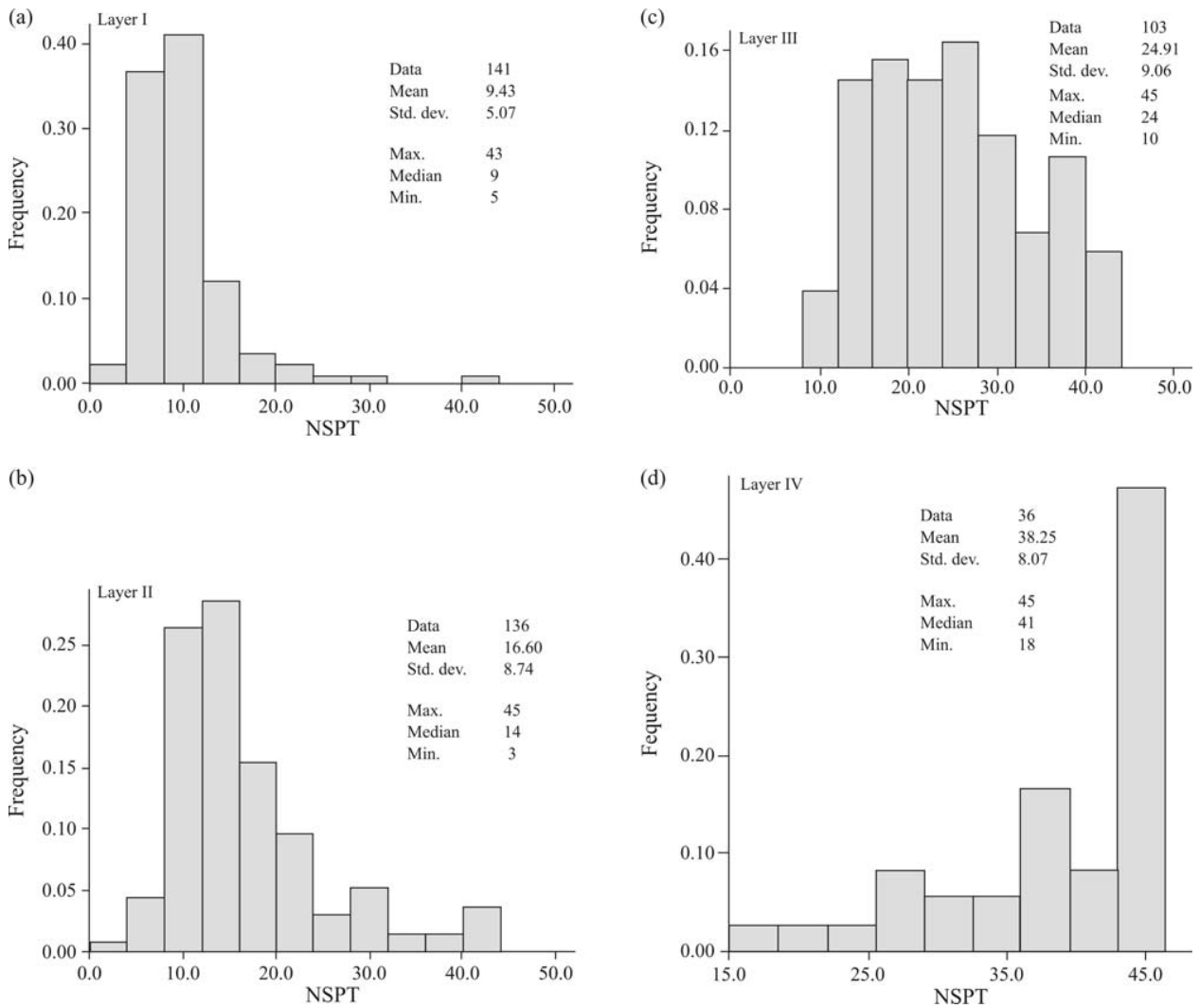


**Figure 5** - Histogram of  $N_{SPT}$  values for layer I (a), layer II (b), layer III (c), and layer IV (d).

$$\gamma(h) = 10 + 55.10 \times Sph \left( \frac{N0^\circ}{547} + \frac{N90^\circ}{775} \right) \quad (4)$$

The terms in the above equations are:

$$\gamma(h) = C_0 + C_1 \times Sph \left( \frac{N0^\circ}{a_1} + \frac{N90^\circ}{a_2} \right) \quad (5)$$

where  $\gamma(h)$  is the variogram,  $C_0$  is the nugget effect,  $C_1$  is the contribution to the sill from the 1<sup>st</sup> spherical model,  $Sph$  is the spherical model,  $a_1$  and  $a_2$  are, respectively, the length of the minor and major axis of anisotropy, and  $N0^\circ$  and  $N90^\circ$ , are, respectively, the azimuths minor and major axis of anisotropy direction.

### 5. Geostatistical Simulation

Geostatistical simulation provides the framework to estimate an unknown value and its associated estimation error. A simulated model is said to be conditionally simulated

if it returns data values at their location, reproducing data statistics and spatial continuity, *i.e.*, the histogram and variogram (Journel, 1974). Conditional simulation is constructed based on Monte Carlo methods (Chilès & Delfiner, 1999). Journel (1974), David (1977), Journel & Huijbregts (1978), and Deutsch & Journel (1998) present theoretical aspects related to the conditional stochastic simulations.

A variable  $Z_s(x)$  is interpreted as a realization of a Random Function (RF) and it is characterized by a distribution function (histogram) and a covariance function or variographic model (variogram). The idea of simulation is to generate several realizations  $z_s(x)$  from the same RF to provide the means to access local and global uncertainty (Journel & Huijbregts, 1978). Each simulated point is represented by a conditional cumulative distribution function (*ccdf*), derived from a model of multivariate distribution function  $Z(x)$ . In each location  $x$ , all distributions functions are specified through mean and variance values.

The principle is that, at each simulated point,  $L$ , equally probable results are generated. The simulation is considered conditional if it matches the data values at their locations. In addition to the distribution be conditioned to the data, each simulated point is randomly visited and its value is added to the dataset. Consequently, the local probability conditional distribution function is not the same for different realizations.

### 5.1 Sequential Gaussian Simulation

The most used stochastic conditional simulation algorithms are the sequential Gaussian (Isaaks, 1990), sequential indicator (Alabert, 1987), and the turning bands method (Matheron, 1973). These algorithms are available in most geostatistical softwares, such as GSLIB (Geostatistical Software's Library) (Deutsch & Journel, 1998) or Isatis®. Amongst the cited methods, the sequential ones, parametric or nonparametric, are preferentially used.

The main difference between these two groups is the procedure used for constructing the uncertainty models (conditional cumulative distribution function - ccdf): parametric vs. nonparametric. Sequential Gaussian simulation (sGs) is based on the multiGaussian formalism (parametric), whereas the sequential indicator simulation (sis) uses the homonym formalism (nonparametric).

The multiGaussian approach assumes that all multivariate distributions of the data follow a Gaussian distribution. Thus, the application of sGs algorithm demands that the experimental distribution of the random variable (RV)  $Z(x)$  follows a Gaussian distribution. That is, the RV  $Z(x)$  must be transformed into a RV  $Y(x)$  standard normal. The multiGaussian hypothesis is very convenient, as it allows the uncertainty models (ccdf) to be obtained from a normal distribution, with mean and variance derived from kriging (Goovaerts, 1996). Thus, the mean and the variance of the ccdf in a given unsampled location,  $x$ , are equal to, respectively, estimate  $y_{SK}^*(x)$  and variance  $\sigma_{SK}^2(x)$  of simple kriging (SK). Then, the ccdf can be modeled as:

$$[G(x; y|n)]_{SK}^* = G\left(\frac{y - y_{SK}^*(x)}{\sigma_{SK}(x)}\right) \quad (6)$$

where  $y$  is a Gaussian value of the domain  $[-\infty; +\infty]$ . The estimated values  $y_{SK}^*(x)$  and  $\sigma_{SK}^2(x)$  are calculated from  $n$  information  $y(x_\alpha)$  ( $\alpha = 1, \dots, n$ ) in the neighborhood of  $x$  (Journel & Huijbregts, 1978, p. 566).

After constructing the ccdf, a simulated datum  $y^{(l)}(x_j)$  is drawn from it via Monte-Carlo simulation. Generally, the following stages are common to all stochastic sequential simulation algorithms (parametric or nonparametric):

(i) definition of a random path, in which each unsampled location  $x_j$  ( $j = 1, \dots, N$ ) (point, cell or block of the grid) is visited only once;

(ii) construction of the uncertainty model (ccdf) at the location  $x_j$  - conditional to the  $n$  experimental information in the neighborhood of  $x_j$ ;

(iii) simulation of a value  $y^{(l)}(x_j)$  from the RV  $Y(x_j)$ , by drawing randomly from the ccdf (Monte-Carlo simulation);

(iv) inclusion of  $y^{(l)}(x_j)$  into the data set, representing an addition to the conditional information to be used in the following  $N$  grid nodes to be visited  $\{y^{(l)}(x_j), j = 1, \dots, N\}$ ;

(v) repetition of the stages (ii) to (iv) until a simulated value is associated to each of the  $N$  locations;

(vi) repetition of the steps (i) to (v) to generate  $L$  equally probable realizations of the spatial distribution of the RV  $Y(x)$ .

Hence, the set  $\{y^{(l)}(x_j), j = 1, \dots, N\}$  represents a realization of the random function (RF)  $Y(x)$  in the physical domain defined by the information  $y(x_\alpha)$  ( $\alpha = 1, \dots, n$ ), in the normal space. Whereas the set  $\{y^{(l)}(x_j), l = 1, \dots, L\}$  represents  $L$  simulations of the RV  $Y$  at location  $x_j$  ( $j = 1, \dots, N$ ). Later, the simulated data set  $\{y^{(l)}(x_j) (j = 1, \dots, N \text{ and } l = 1, \dots, L)\}$  is transformed to the original space of the RV  $Z(x)$ . Therefore, the value of the RV  $Z$  at each location  $x_j$  ( $j = 1, \dots, N$ ) is simulated within the domain of variation of the RV  $Z(x)$ , through a random procedure, from the ccdf. At each location, the simulation process generates a distribution, composed of  $L$  values. That distribution can be considered a numerical approach of the ccdf, *i.e.*:

$$F(x; z|n) \approx \frac{1}{L} \sum_{l=1}^L i^l(x; z) \quad (7)$$

where  $F(x; z|n)$  represents the probabilities assumed by the ccdf at each location  $x_j$  ( $j = 1, \dots, N$ ) and  $i^l(x; z)$  is an indicator variable as follows:

$$i^l(x; z) = \begin{cases} 0 & \text{if } Z^l(x) \leq z \text{ with } l=1, \dots, L \\ 0 & \text{if not} \end{cases} \quad (8)$$

Sequential Gaussian simulation is based on the multivariate normal random function model, which follows the Bayes theorem. It is demonstrated that there exists equivalence between an image generated from a multivariate distribution function and that generated from the sequence of univariate conditional distribution functions (Olea, 1999). The sequential Gaussian simulation (sGs) algorithm was applied to this dataset and results are hereinafter depicted.

### 5.2 Analysis of $N_{SPT}$ variability

Every time one interpolates any geological or geotechnical attribute at a non-sampled location, given the information (boreholes) in the local vicinity of the grid node being interpolated, there is an error associated with this estimate. It would be reasonable to assume that the engineer responsible for the foundation design should have an estimate map with the geotechnical properties relevant for his/her project, combined with an error assessment (uncertainty associated with the estimates). These errors are asso-

ciated with (Phoon & Kulhawy, 1999): (i) soil inherent spatial variability, due to variation in formation conditions and stress history from one point to another in space; (ii) measurement errors, due to insufficient control of testing procedure and equipment; (iii) deterministic trends in soil properties, such as the increase in soil strength with depth due to the confining increase in pressure; and (iv) the collection of field data over long time periods.

Following this rationale, the assessment of the error associated with the estimation of geotechnical properties (soil strength) using sGs is proposed here. In addition, this error should be incorporated in risk analysis along the decision-making process.

The foundation project requires soil-bearing capacity and the safety factor used in this project is associated with the degree of certainty one has on the soil properties selected. With the proposed procedure to quantify this uncertainty, the choice of safety factor can be conducted in a less arbitrary way. In addition, by mapping areas of high uncertainty in soil-bearing capacity, one can locate extra sampling points, in order to reduce locally the uncertainty, if necessary.

Fifty equally possible scenarios were generated at 100 x 100 m<sup>2</sup> grid. This grid is in accordance with the average panel size used for city planning at the location selected for this case study. To obtain a panel simulation, *a posteriori* change of support was used, averaging all point nodes simulated within the domain of a panel.

A perfect reproduction of histograms and variograms by the simulated models is unattainable due to uncertainties in the input statistics. The models should exhibit ergodic fluctuations, and there are some factors which control the magnitude of this fluctuation. Figure 6 shows ergodic fluctuations for the variogram using data on normal space. In order to illustrate the discussed methodology, only the results from soil layer III are depicted in this paper. The realizations generated by simulation were also checked for univariate statistics reproduction, and it was found that the ergodic RF model supports the statistics of the normalized input data (Figs. 7 a, b and c).

Figure 8 shows the distribution maps of the average (E-type) of N<sub>SPT</sub> values simulated at each panel from layer III. These E-type models are similar to models generated by kriging (Zingano *et al.*, 1996; Costa, 1997; Goovaerts, 1997).

The simulation of N<sub>SPT</sub> distribution for all soil layers ultimately aims at estimating the soil properties and its uncertainty, incorporating it into the foundation design. For instance, layer I comprises values of N<sub>SPT</sub> capable of supporting shallow foundations, whereas layers II, III, and IV are capable of bearing deep foundation.

Maps of local variability for N<sub>SPT</sub> values are selected as an important tool for uncertainty assessment in foundation projects. There are several methods to evaluate and visualize these local uncertainties from the conditional sim-

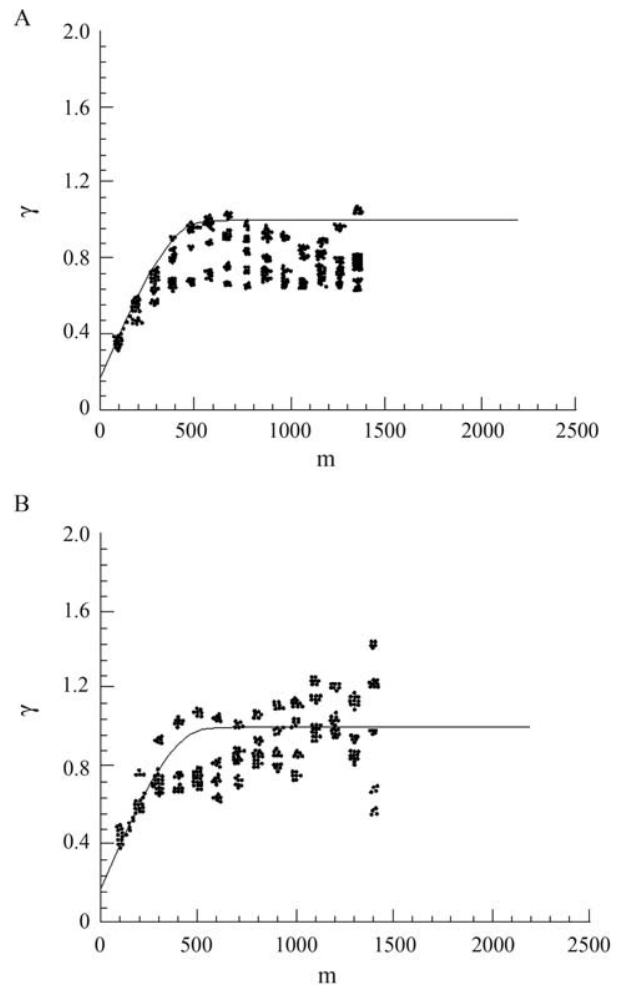


**Figure 6** - Variograms of normalized data (layer III - solid line) showing ergodic fluctuation (dots) at the principal directions of spatial continuity (a) 0° and (b) 90°.

ulation realizations (Srivastava, 1994; Goovaerts, 1997). An uncertainty measure was adopted for the present study, which is the coefficient of variation (CV) for N<sub>SPT</sub> value at each panel.

The maps for CV in each soil layer are presented in Fig. 9. The values of CV are obtained according to Eq. (9):

$$CV_{bl} = \frac{\sigma_s}{\bar{X}_s} \tag{9}$$

where  $CV_{bl}$  is the panel-by-panel coefficient of variation;  $\sigma_s$  is the standard deviation of the fifty simulated values at each panel; and  $\bar{X}_s$  is the mean of these fifty values (E-type).

Maps for the CV show that central region of layers I and III (Figs. 9a and 9c) present low CV values, approximately 20%. This area is densely sampled, consequently showing a lower level of uncertainty compared with the remaining sectors. Layer IV (Fig. 9d) has CV values of

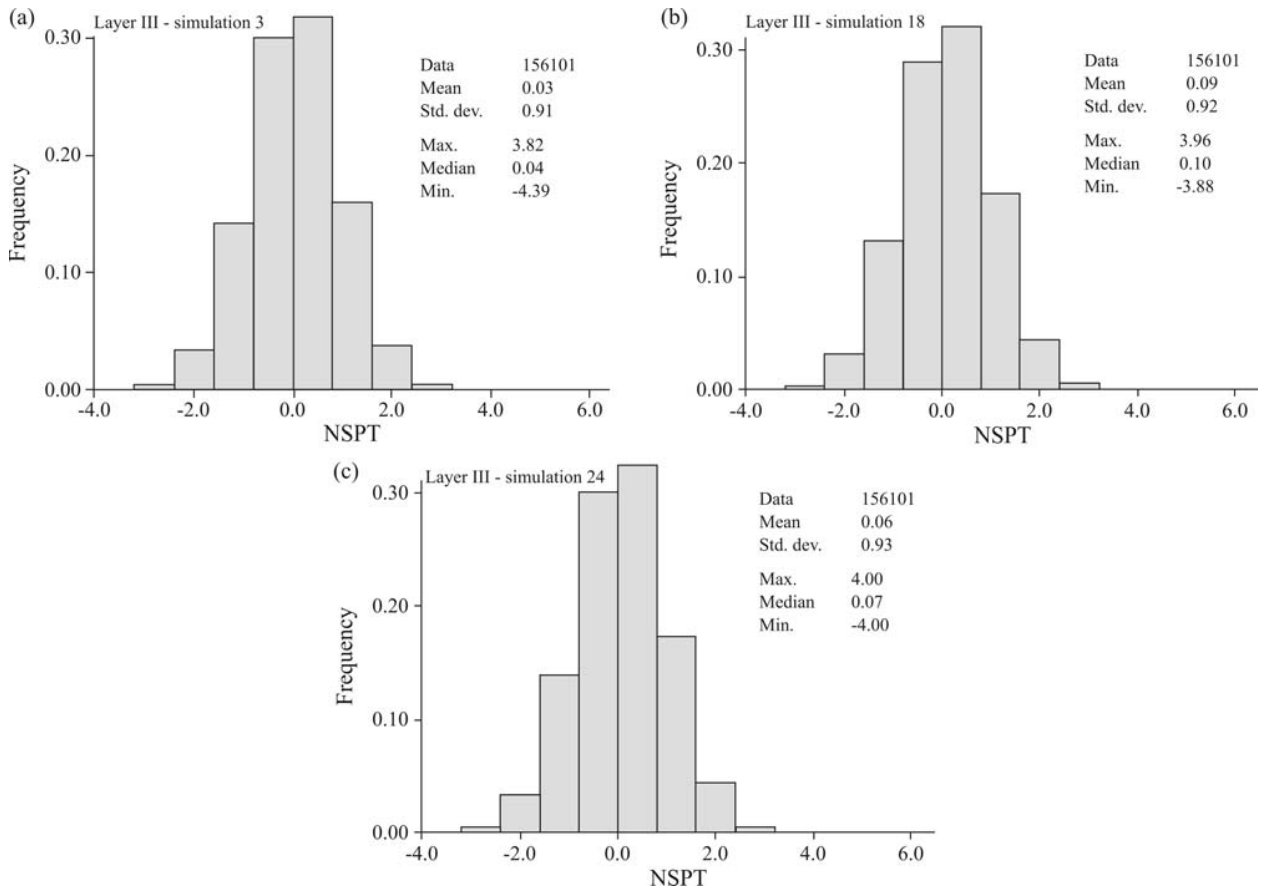


**Figure 7** - Histograms of simulated models (normal space) selected randomly among 50 realizations. Layer III - simulation 3 (a), 18 (b) and 24 (c).

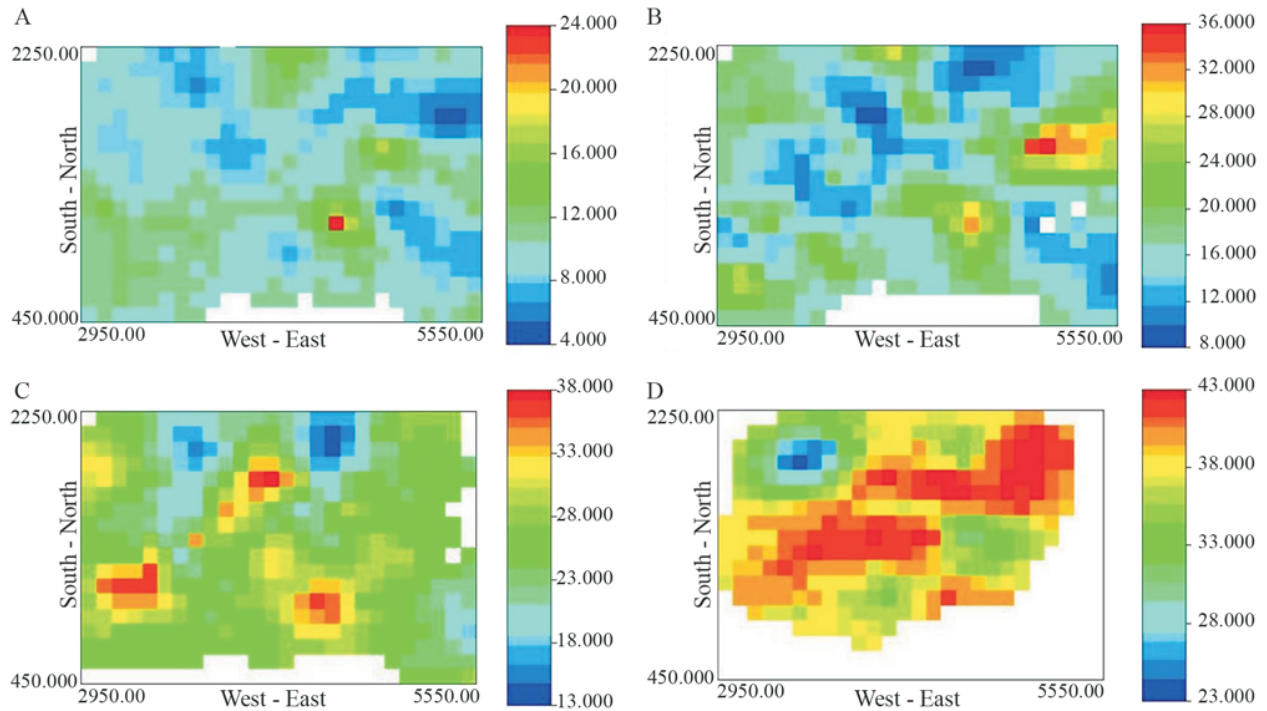


**Figure 8** - Images showing the mean  $N_{SPT}$  value (E-type) at each panel (a) layer I, (b) layer II, (c) layer III, and (d) layer IV.

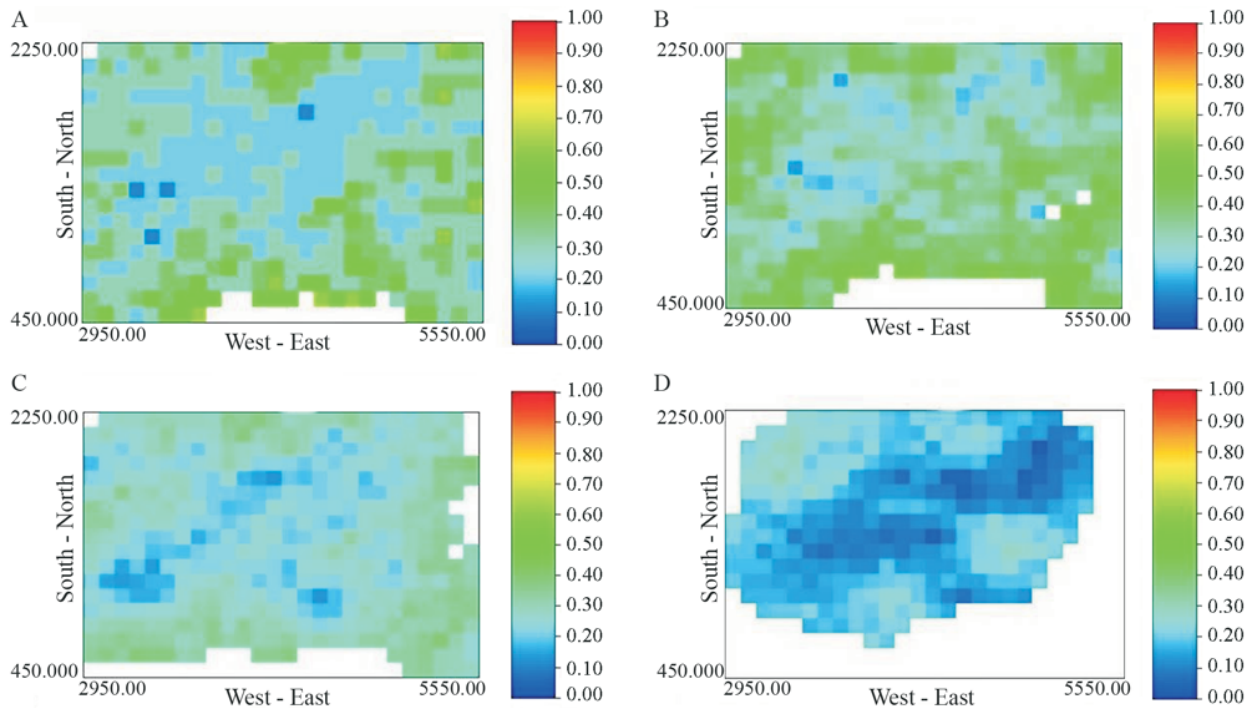


**Figure 9** - Variability map measured by the coefficient of variation (CV) at each panel for  $N_{SPT}$  values (a) layer I, (b) layer II, (c) layer III, and (d) layer IV.

approximately 10% at the same central area and in the remaining regions the values are approximately 20%. Layer II (Fig. 9b) has higher variability than the other three layers, reaching 50% in the most extreme zones. On average, the variability ranges from 20% to 40% in the central area of layer II.

Layer II has higher variability than the others, possibly due to its transitional characteristics described previously. This layer is also the region where water level was detected frequently, which reduces soil strength followed by an increase in the next dried zone. The relevance in identifying variability in soil properties is presented in various papers (Soulié *et al.*, 1990; Folle, 2002 e Elkateb *et al.*, 2003). Geotechnical engineers are willing to improve the geotechnical investigation optimizing the whole process including: development of better survey methods, reduction of the period taken for the survey, better definition of the number of sampling points, and consequently reduction of the costs involved. Following this interest, this paper introduced a methodology that can quantify the spatial variability of soil geotechnical properties to corroborate with these needs.

## 6. Conclusions

Several stochastic simulations were generated and were used to evaluate uncertainty due to variability related to  $N_{SPT}$  values at different soil layers. Sequential Gaussian simulations proved to be an adequate tool to assess uncertainty associated to  $N_{SPT}$  estimate. sGs was used to generate

equally likely scenarios which after combination could facilitate global and local error measurements. In this study, only  $N_{SPT}$  values were mapped; however, other correlated soil resistance measures or even other geotechnical properties could also be used.

Fluctuations around the mean estimated values (E-type) provide the means to evaluate the confidence intervals on interpolated results. In addition, the methodology can be used for planning infill drilling at zones of higher uncertainty in case risk reduction is desirable.

## References

- ABNT (1982) Identification and Description of Samples of Soil Obtained from Surveys of Simple Recognition. Brazilian Standard NBR 7250, Rio de Janeiro, 5 pp. (in Portuguese).
- ABNT (1999) Implementation of Surveys of Simple Recognition of the Soil (SPT). Brazilian Standard NBR 6484, Rio de Janeiro, 12 pp. (in Portuguese).
- Alabert, F.G. (1987) Stochastic Imaging and Spatial Distributions Using Hard and Soft Information. Master's Thesis, Applied Earth Science Department, Stanford University, 197 pp.
- Armstrong, M. (1998) Basic Linear Geostatistics. Springer, Berlin, 153 pp.
- Attanasi, E.D. & Coburn, T.C. (2004) A bootstrap approach to computing uncertainty in inferred oil and gas reserve estimates. *Natural Resources Research*, 13:1, p. 45-52.

- Chilès, J.P. & Delfiner, P. (1999) *Geostatistics: Modeling Spatial Uncertainty*. Wiley-Interscience, New York, 695 pp.
- Costa, J.F. (1997) *Developments in Recoverable Reserves and Ore Body Modeling*. PhD Thesis, WH Bryan Mining Geology Research Centre, The University of Queensland, 333 pp.
- Costa, J.F.C.L. & Koppe, J.C. (1999) Assessing uncertainty associated with the delineation of geochemical anomalies. *Natural Resources Research*, 8:1, p. 59-67.
- David, M. (1977) *Geostatistical Ore Reserve Estimation*. *Developments in Geomathematics 2*. Elsevier Scientific Publishing Company, Amsterdam, 364 pp.
- Deutsch, C.V. & Journel, A.G. (1998) *GSLIB: Geostatistical Software Library & User's Guide*. Oxford University Press, New York, 369 pp.
- Elkateb, T.; Chalaturnyk, R. & Robertson, P.K. (2003) An overview of soil heterogeneity: quantification and implications on geotechnical field problems. *Canadian Geotechnical Journal*, 40:1, p. 1-15.
- Folle, D. (2002) *O Estudo Geoestatístico de Sondagens Spt para Geração de Mapas Auxiliares em Obras de Engenharia*. Dissertação de Mestrado, Escola de Engenharia, Universidade Federal do Rio Grande do Sul, Porto Alegre, 217 pp.
- Folle, D. (2003) *Study of the Soil Resistance Using the Standard Penetration Test in Passo Fundo City, South of Brazil*. Centre de Géostatistique de Fontainebleau, France, 70 pp.
- Goovaerts, P. (1996) Accounting for local uncertainty in environmental decision making processes. In: *Proceedings of the Fifth International Geostatistics Congress*, Wollongong, Kluwer Academic Publishers, v. 2, p. 929-940.
- Goovaerts, P. (1997) *Geostatistics for Natural Resource Evaluation*. Oxford University Press, New York, 464 pp.
- Isaaks, E.H. & Srivastava, M.R. (1989) *An Introduction to Applied Geostatistics*. Oxford University Press, New York, 552 pp.
- Isaaks, E.H. (1990) *The Application of Monte Carlo Methods to the Analysis of Spatially Correlated Data*. Ph.D. Thesis, Applied Earth Science Department, Stanford University, 213 pp.
- Journel, A.G. & Huijbregts, C.J. (1978) *Mining Geostatistics*. Academic Press, London, 600 pp.
- Journel, A.G. (1974) Geostatistics for conditional simulation of ore bodies. *Economic Geology*, 69:5, p. 673-687.
- Leuangthong, O.; McLennan, J.A. & Detsch, C.V. (2004) Minimum acceptance criteria for geostatistical realizations. *Natural Resources Research*, 13:3, p. 131-141.
- Matheron, G. (1963) Principles of geostatistics. *Economic Geology*, 58:8, p. 1246-1266.
- Matheron, G. (1973) The intrinsic random functions and their applications. *Journal for Applied Probability*, v. 5, p. 439-468.
- Morgenstern, N.R. (2000) Performance in geotechnical practice. *The Inaugural Lumb Lecture*. Transactions, Hong Kong Institution of Engineers, v. 7, 59 pp.
- Naime, R. (1999) *Uso das Sondagens à Percussão e Sondagens Penetrométricas na Investigação dos Solos - Estimativa da Capacidade de Carga dos Solos de Porto Alegre e Passo Fundo*. Qualificação de Doutorado, Departamento de Geociências, Universidade Federal do Paraná, 417 pp.
- Olea, R.A. (1999) *Geostatistics for Engineers and Earth Scientists*. Kluwer Academic Publishers, Norwell, 302 pp.
- Phoon, K.K. & Kulhawy, F.H. (1999) Characterization of geotechnical variability. *Canadian Geotechnical Journal*, v. 36:4, p. 612-624.
- Pilger, G.G. (2000) *Crítérios para Locação Amostral Baseados em Simulação Estocástica*. Dissertação de Mestrado, Escola de Engenharia, Universidade Federal do Rio Grande do Sul, Porto Alegre, 127 pp.
- Pilger, G.G.; Costa, J.F.C.L. & Koppe, J. (2001) Additional Samples: Where They Should Be Located. *Natural Resources Research*, 10:3, p. 197-207.
- Pinto, C.S. (2000) *Curso Básico de Mecânica dos Solos em 16 Aulas*. Oficina de Textos, São Paulo, 247 pp.
- Projeto RADAMBRASIL (1986) *Mapa Geológico*. Folhas SH/SI.22/21\*. Esc:1.100.000, v. 33.
- Soulié, M.; Montes, P. & Silvestri, V. (1990) Modelling spatial variability of soil parameters. *Canadian Geotechnical Journal*, 27:5, p. 617-630.
- Souza, L.E. de; Costa, J.F.C.L. & Koppe, J. (2004) Uncertainty estimate in resources assessment: a geostatistical contribution. *Natural Resources Research*, 13:1, p. 1-15.
- Srivastava, R.M. (1994) The visualization of spatial uncertainty. In: *Stochastic Modeling and Geostatistics, Principles, Methods and Case Studies*. AAPG Computer Applications in Geology, Tulsa, pp. 339-345.
- Sturaro, J.R. & Landim, P.M.B. (1996) *Mapeamento geoestatístico de ensaios de penetração padronizada (SPT)*. Solos e Rochas, v. 19:1, p. 3-14.
- Zingano, A.C.; Costa, J.F.C.L. & Koppe, J.C. (1996) Conditional simulation for oil grade estimation and mine planning. *Proc. 5<sup>th</sup> International Symposium on Mine Planning and Equipment Selection*, São Paulo, pp. 97-102.